Comparison of Complex Potentials: Absorption Width and Robustness†

J. P. Palao and J. G. Muga*

Departamento de Física Fundamental y Experimental, Facultad de Física, Universidad de La Laguna, Tenerife, Spain

Received: April 21, 1998; In Final Form: July 15, 1998

Virtues and weaknesses of several complex absorbing potentials are examined. In particular, we study the absorption width and robustness of different optimized absorbing potentials for two types of boundary conditions. It is found that "composite potentials" formed by addition of square barrier units provide a flexible, robust, and efficient approach to absorb in the low momentum region, where other potentials are useless.

1. Introduction

Absorbing complex potentials are an important tool in different numerical methods used to study quantum reactive collisions (stationary and time-dependent) and cumulative reaction probabilities;[1−5] see additional references in a recent review.[6] Several works have been devoted to analysis of general properties of complex potentials as well as the behavior of specific functional forms.[1,7−12] This paper complements these works by comparing, for two different types of boundary conditions, the robustness and the effective absorption range of some of these functional forms: monomial potentials, the family of potentials proposed by Brouard, Macías, and Muga in refs 9 and 10 and their generalizations, and composite potentials formed by addition of square barriers. The numerical examples provided should also clarify some common misconceptions about complex absorbing potentials.

Throughout the paper we shall limit the discussion to one dimension (it may be, for example, one of the scaled Jacobi coordinates in a collinear atom−diatom collision). To analyze and compare the performance of absorbing potentials ν of finite support $[0, L]$, it is helpful to use dimensionless quantities. Dividing the stationary Schrödinger equation for a state of energy $E = p^2/(2m)$,

$$H(y)\Psi(y) = -\frac{\hbar^2}{2m}\frac{\mathrm{d}^2}{\mathrm{d}y^2}\Psi(y) + \nu(y)\Psi(y) = E\Psi(y) \quad (1)$$

by $\lambda L^{-1/2}$, where $\lambda = \hbar^2/2mL^2$, and using the dimensionless potential and total energies $V = \nu/\lambda$ and $E = E/\lambda$, respectively, all potentials have support $[0, 1]$ in the dimensionless coordinate $x = y/L$. The dimensionless Schrödinger equation takes the form

$$-\frac{\mathrm{d}^2}{\mathrm{d}x^2}\psi(x) + V(x)\psi(x) = k^2\psi(x) \quad (2)$$

where $\psi(x) = L^{1/2}\Psi(y)$, and $k = E^{1/2} = pL/\hbar$ is a dimensionless wavenumber (we shall also frequently refer to k as a "momentum"). The performance of a complex potential as an absorber for incidence from the left is defined by its *nonabsorption* or *survival* probability, the sum of transmission and reflection probabilities, $S(k) \equiv |T^{\mathrm{l}}(k)|^2 + |R^{\mathrm{l}}(k)|^2$. ($T^{\mathrm{l}}$ and R^{l} are the complex transmission and reflection amplitudes for left incidence.) The absorption for a wave packet can be obtained by averaging $1 - S(k)$ with the initial momentum distribution. However, these theoretical absorption values may be difficult to achieve in an actual calculation because, due to the space discretization imposed by grid methods, the potential is only sampled at a limited set of points. If the potential oscillates wildly, a large number of grid points may be necessary to reproduce in the numerical calculation its ideal absorption curve. A potential is defined to be "robust" if it maintains its theoretical absorption when discretized. In general, the *robustness* will vary with incident momentum. A robustness parameter will be defined later to quantify this concept.

The ideal "all-purpose" absorbing potential for an arbitrary application would absorb fully all incident momenta

$$S(k) = 0 \qquad (\text{all } k > 0) \quad (3)$$

and be as robust as possible. These ideal properties are not satisfied entirely by any known potential, and it is important to keep searching for better functional forms in order to study accurately, with a minimum of grid points, reactive problems where broad momentum intervals are represented. The low k region is very important in practice because the potential should occupy a small (dimensional) interval $[0, L]$ to minimize the computational effort. But the dimensionless variable k depends linearly on L and on the dimensional momentum p, so that this objective can only be fulfilled with good absorbers at low values of k.

In section 2 the different potentials are described, and their performance is compared in section 3. The paper ends with the main conclusions drawn from the numerical results.

2. Potentials

Since the complex potentials are used in many different applications that use several numerical techniques, it is useful to distinguish and study two types of potentials. (a) Type I potentials include an infinite barrier:

$$V_{\mathrm{I}}(x) = \begin{cases} 0 & \text{if } x < 0 \\ W_{\mathrm{I}}(x) & \text{if } 0 \le x \le 1 \\ \infty & \text{if } 1 < x \end{cases} \quad (4)$$

Because of the infinite wall there is no transmission in this case. Type I potentials are naturally adapted to Dirichlet homogeneous boundary conditions (vanishing wave function at the edges of

* Corresponding author. E-mail JMUGA@ULL.ES. Fax 34-22-603684.

† It is a pleasure to dedicate this article to Raphy Levine on the occasion of his 60th birthday.

10.1021/jp981943+ CCC: $15.00
Published on Web 10/17/1998

the "box"). (b) Type P potentials do not have an infinite wall, so they are instead suitable for periodic boundary conditions:

$$V_{\mathrm{P}}(x) = \begin{cases} 0 & \text{if } x < 0 \\ W_{\mathrm{P}}(x) & \text{if } 0 \le x \le 1 \\ 0 & \text{if } 1 < x \end{cases} \quad (5)$$

Note that the same function $W(x)$ may lead to different values of the survival $S(k)$ for types I and P.

The traditional approach is to use a purely imaginary functional form with parameters that can be varied to obtain maximum absorption at or around a selected value k_0. Many of the potential forms proposed have the factorized form

$$W(x; k_0) = -i\eta(k_0)F(x) \quad (6)$$

so that for a fixed $F(x)$ function, $\eta(k_0)$ is chosen to minimize $S(k_0)$. In order to optimize the potentials at every k_0, the Schrödinger equation is solved numerically to determine the complex transmission and reflection amplitudes, $T^{\mathrm{I}}(k_0)$ and $R^{\mathrm{I}}(k_0)$. In this work a quasi-Newtonian method has been used to find the best value of $\eta(k_0)$.

2.1. Powers of *x*. The most common particular case of eq 6 is the monomial form:

$$W(x; k_0) = -i\eta(k_0)x^{\mathrm{n}} \quad (7)$$

In particular we shall limit our study to $n = 1$ and $n = 2$ and consider purely real or complex prefactors (η_{LR} or η_{LC} for the linear case, and η_{QR} or η_{QC} for the quadratic case),

$$W_{\mathrm{LR}}(x; k_0) = -i\eta_{\mathrm{LR}}(k_0)x \quad (8)$$

$$W_{\mathrm{LC}}(x; k_0) = -i\eta_{\mathrm{LC}}(k_0)x \quad (9)$$

$$W_{\mathrm{QR}}(x; k_0) = -i\eta_{\mathrm{QR}}(k_0)x^2 \quad (10)$$

$$W_{\mathrm{QC}}(x; k_0) = -i\eta_{\mathrm{QC}}(k_0)x^2 \quad (11)$$

When necessary, an additional subscript I or P will specify the potential type (otherwise it may be understood that the two types are being considered). Even though V_{QR} and V_{LR} are particular cases of V_{QC} and V_{LC}, we have optimized the two forms separately in the numerical comparisons, since in most of the applications, only η real has been used.

Riss and Meyer have extensively studied the properties of type P potentials with the general form eq 7 but for real prefactors η. They found that higher powers ($n > 2$) improve the performance of linear or quadratic potentials only for large k_0, but the differences are not significant. (The error made by discretizing the potentials is generally larger than the change in absorption due to increasing n.) We have found the same behavior for complex η, and also for type I potentials (with real or complex η), so that the linear and/or quadratic potentials may be taken as representative cases. Their low-energy behavior will be discussed in section 3.1.

2.2. Generalizations of the Construction Method of Brouard, Macías, and Muga. A different strategy was proposed in refs 9 and 10, based on a simple inversion method that assumes first a functional form *of the wave function* in the potential region. In this manner a family of potentials $V^{(\nu)}_{\mathrm{BMM}}$ can be generated to systematically increase the absorption widths. The basic ideas are first outlined, and then several generalizations are provided.

The simplest functional form of the wave function is a polynomial:

$$\psi(x) = \sum_{j=0}^{J} a_j(k_0)x^j \quad (12)$$

where the complex coefficients a_j are obtained by imposing $J + 1$ conditions at the boundaries $x = 0$ and $x = 1$. In particular, by choosing $R(k_0) = 0$ (no reflection for k_0), and putting an infinite wall at $x = 1$ to completely avoid transmission, the three conditions ($J = 2$) read

$$\psi(x = 0) = 1$$

$$\frac{\mathrm{d}}{\mathrm{d}x}\psi(x = 0) = ik_0$$

$$\psi(x = 1) = 0 \quad (13)$$

Substituting eq 12 into eq 13 leads to a system of equations that can be solved for the coefficients a_j. The potential is then obtained by solving for $W(x)$ in the Schrödinger equation:

$$W^{(0)}_{\mathrm{BMM,I}}(x) = k_0^{\,2} + \frac{\psi''(x)}{\psi(x)} = k_0^{\,2} + 2(x-1)^{-1}\left(x + \frac{1}{1+ik_0}\right)^{-1} \quad (14)$$

The main virtue of this method is that it provides an explicit potential that guarantees full absorption for any selected momentum (also for an arbitrary length L when dimensional quantities are used), and this may be sufficient for some applications. This zeroth-order potential also makes clear that the complex potentials can improve their absorption by adding a real part, that discontinuities do not preclude full absorption, and that (when dimensional units are used) the absorption can be achieved in an arbitrarily short interval L (contrast this to the semiclassical, but generally invalid, notion that several wavelengths are required).

Higher order members of this family of potentials can be constructed by imposing that successive derivatives of $R^{\mathrm{I}}(k)$ become zero at $k = k_0$. For type I potentials, if ν derivatives are made zero, then $J = 2 + \nu$. Except for $\nu = 0$, the coefficients a_j have to be obtained numerically and, in practice, going beyond $\nu = 2$ is cumbersome.

The same method can be adapted to type P potentials. Now $R^{\mathrm{I}}(k_0) = T^{\mathrm{I}}(k_0) = 0$, and the continuity of the wave function derivative at $x = 1$ imposes the additional condition

$$\frac{\mathrm{d}}{\mathrm{d}x}\psi(x = 1) = 0 \quad (15)$$

In this manner the explicit form of a zeroth-order type P potential absorbing completely at k_0 is

$$W^{(0)}_{\mathrm{BMM,P}}(x) = k_0^{\,2} + 6\left[x - \frac{3+2ik_0}{3(2+ik_0)}\right]\left(x + \frac{1}{2+ik_0}\right)^{-1}(x-1)^{-2} \quad (16)$$

To extend the effective absorption width, successive derivatives of T^{I} and R^{I} at $k = k_0$ are made zero, so for each additional order two more coefficients are needed (for type P potentials $J = 3 + 2\nu$).

The method can be also generalized to absorb at an arbitrary number of k points by using the interferences between contigu-

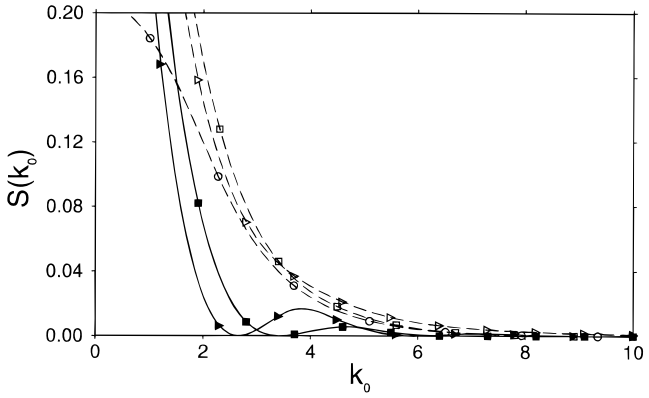

Figure 1. Survival for optimized potentials, $S(k_0)$, versus k_0. Dashed lines (and open symbols) correspond to type P potentials, whereas solid lines (and solid symbols) correspond to type I potentials in all figures. Squares, V_{QR}; circles, V_{QC}; triangles right, V_{LR}. For all other potentials discussed in the text, $S(k_0)$ is indistinguishable with the real axis in the scale of the figure.

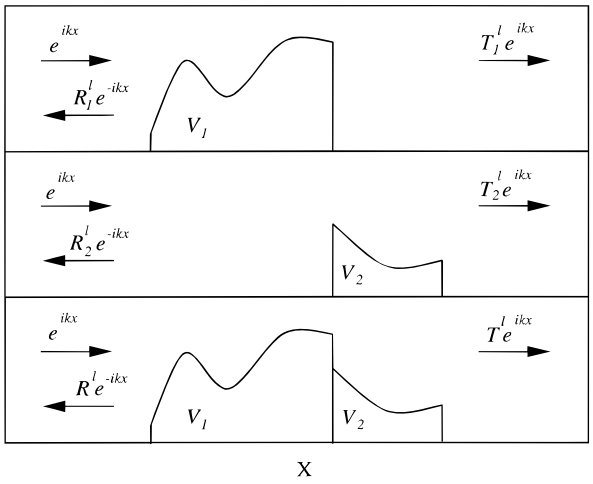

Figure 2. Two arbitrary contiguous potential units V_1 and V_2 and the composite barrier $V_1 + V_2$, with the corresponding reflection and transmission amplitudes for left incidence.

ous potential units.[13] Assume first that two complex potential units V_1 and V_2 have contiguous and finite supports, as depicted in Figure 2. Let $T^{r,l}$ and $R^{r,l}$ be the complex transmission and reflection amplitudes for right (r) and left (l) incidence of the compound potential $V = V_1 + V_2$, and $T_i^{r,l}$ and $R_i^{r,l}$, $i = 1, 2$, the partial amplitudes of the potential units. From the dependence of $T^{r,l}$ and $R^{r,l}$ on the partial amplitudes it is possible to establish the following conditions so that the compound potential absorbs two different momenta k_1 and k_2 (here $k = d_1 p/\hbar$ where d_1 is the dimensional width of the first barrier):[13]

$$T_1^{l}(k_1) = R_1^{l}(k_1) = 0 \tag{17}$$

$$T_2^{l}(k_2) = 0 \tag{18}$$

$$R_2^{l}(k_2) = \frac{R_1^{l}(k_2)}{R_1^{l}(k_2)R_1^{r}(k_2) - T_1^{l}(k_2)T_1^{r}(k_2)} \tag{19}$$

Note that V_1 absorbs k_1, and so does V, but V_2 does not absorb at k_2. Instead, an interference effect is responsible for the absorption of k_2 by V. To fulfill these equations V_1 can be constructed with eq 16, while V_2 may be obtained by imposing eqs 18 and 19 on an assumed form of the wave function. This

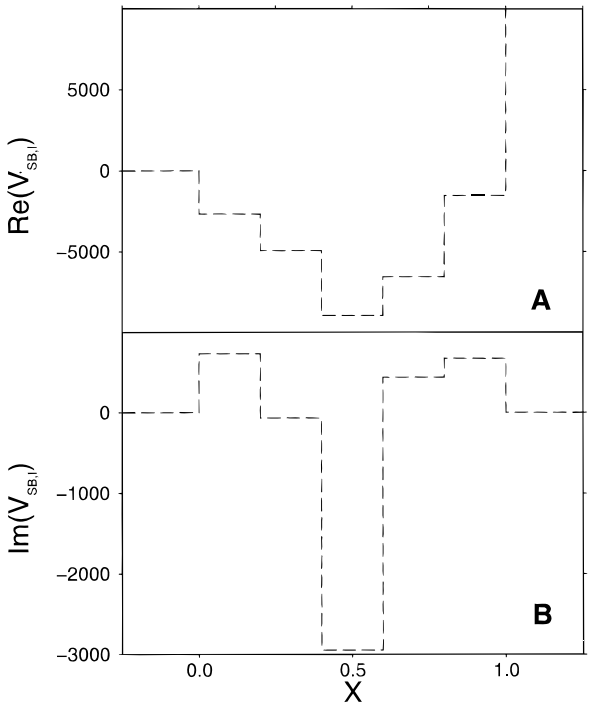

Figure 3. Real and imaginary parts of a particular composite barrier potential $V_{SB,I}$, $N = 5$. The parameters are given in Table 1.

leads to four conditions that can be satisfied, for example, by a cubic polynomial. The addition of new units (V_3, V_4, ...) can be continued in the same fashion to absorb *in principle* an arbitrary number of values of k (for each new unit conditions similar to eqs 18 and 19 are imposed). Unfortunately, we have not been able to exploit this method efficiently in practice, because small numerical errors in the calculation of the partial reflection and transmission amplitudes for the unit V_j tend to blow up when the reflection amplitude for V_{j+1} is calculated by means of eq 19, if $T_j(k_{j+1})$ is very small. Thus, unless a way is found to circumvent this problem (possibly by using other functional forms for the wave function and potential units), their applicability as a computational tool is limited. However, in the next subsection a numerically robust alternative also making use of the interferences of composite barriers, but in a less explicit and more effective way, is provided.

2.3. Composite Potentials Formed by Adding Square Barrier Units. In general, the absorption in a given interval $[k_1, k_2]$ will improve by increasing the number of optimization parameters of the functional form of the complex potential. However, for arbitrary functional forms the numerical optimization can be a lengthy process that requires solving the Schrödinger equation many times, so that the number of free parameters is usually limited to one or two. A more flexible way out is provided by using a composite potential V_{SB} formed by adding a series of contiguous N complex square barriers of length $\epsilon = 1/N$ and complex energies $\{V_j\}$, $j = 1, 2, ..., N$. An example is provided in Figure 3. The solution of the Schrödinger equation in this case involves simply the multiplication of 2×2 transfer matrices,[14] a very fast procedure that allows optimization of many more parameters (two for each barrier) than for any other functional form. To implement the method let us first define the auxiliary matrix $M(k, x)$ by[14]

$$M_{1,1} = \mathrm{e}^{ikx} \qquad M_{1,2} = \mathrm{e}^{-ikx}$$

$$M_{2,1} = k\mathrm{e}^{ikx} \qquad M_{2,2} = -k\mathrm{e}^{-ikx}$$

and the matrix $K(k_j, \epsilon)$ for the jth barrier as

$$K_{1,1} = \frac{e^{k_j\epsilon} + e^{-k_j\epsilon}}{2} \qquad K_{1,2} = \frac{-e^{k_j\epsilon} + e^{-k_j\epsilon}}{2k_j} \tag{20}$$

$$K_{2,1} = \frac{k_j(-e^{k_j\epsilon} + e^{-k_j\epsilon})}{2} \qquad K_{2,2} = \frac{e^{k_j\epsilon} + e^{-k_j\epsilon}}{2} \tag{21}$$

where $k_j = (V_j - E)^{1/2}$. The transfer matrix W relates the coefficients $A_{l,r}$ and $B_{l,r}$ that multiply e^{ikx} and e^{-ikx} on both sides of the barrier ("left" and "right"):

$$\begin{pmatrix} A_l \\ B_l \end{pmatrix} = W \begin{pmatrix} A_r \\ B_r \end{pmatrix} \tag{22}$$

W takes the form

$$W = M^{-1}(k, x = 0)\,[\prod_{j=1}^{N} K(k_j, \epsilon)]\,M(k, x = 1) \tag{23}$$

and the reflection and transmission amplitudes for left incidence are given by

$$R^{l}(k) = \frac{W_{2,1}}{W_{1,1}} \qquad T^{l}(k) = \frac{1}{W_{1,1}} \tag{24}$$

so the survival $S(k)$ or its gradient with respect to variations of the parameters V_j are easily evaluated. The optimization of the potential barriers may be carried out by minimizing with respect to the V_j the sum of the survival probabilities at s values of k evenly spaced in the absorption interval $[k_i, k_f]$:

$$f(V_1, ..., V_N; k_1, ..., k_s) = \sum_{\alpha=1}^{s} S(V_1, ..., V_N; k_\alpha) \tag{25}$$

By increasing the number of barriers N, the flexibility of the potential function increases, and the value of the minimized f decreases. In applications N is chosen according to the density of grid points of the spatial discretization (so that an integer number of grid points corresponds to each barrier, this aspect will be discussed further in the next section). By increasing s the survival curves tend to become flat and close to zero in the full absorption interval $[k_i, k_f]$. An application of this approach to the collinear reaction $H + H_2$[15] shows how the spatial region devoted to absorption is significantly reduced with respect to other potentials, allowing numerical access to low-energy scattering.

3. Comparison

Here a numerical comparison of the performance of the potentials described in the previous section is provided. The three aspects studied are (1) optimized survival at fixed k_0, (2) absorption width, and (3) robustness versus discretization. For the nonspecialist who wants to skip the detailed analysis of the numerical results, a brief summary with the essential conclusions is provided in the next section. To facilitate the interpretation of the figures, the same symbols are used throughout for the same potentials. Thus, dashed lines (with open symbols) correspond to type P potentials, and solid lines (with solid symbols) correspond to type I potentials. The correspondence between symbols and potentials is as follows: Triangles up, $V^{(2)}_{BMM}$; triangles down, $V^{(0)}_{BMM}$; squares, V_{QR} (quadratic with real η); circles, V_{QC} (quadratic with complex η); diamonds, V_{SB} (composite square barriers); triangles right, V_{LR} (linear with real η).

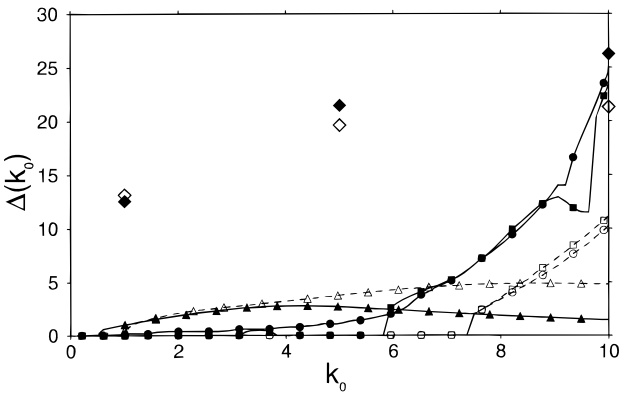

Figure 4. Absorption width $\Delta(k_0; 0.001)$ versus k_0. Diamonds, V_{SB} (5 square barriers); triangles up, $V^{(2)}_{BMM}$; squares, V_{QR}; circles, V_{QC}.

3.1. Minimized Survival. We shall first compare the survival $S(k_0)$ for potentials optimized at every k_0 value; see Figure 1. (Every k_0 point in Figure 1 corresponds to different optimized potential parameters.) A number of optimized potentials provide excellent absorptions for a selected momentum, and their survivals are indistinguishable with the k_0 axis in the scale of this figure. It has been already pointed out that V_{BMM} potentials can always be adapted to guarantee full absorption at any momentum. Actually the results for $V_{LC,I}$, $V_{QC,I}$, V_{BMM}, $V_{SB,P}(N = 2)$, and $V_{SB,I}(N = 1)$ (not shown) are all good enough for all practical purposes in the monochromatic limit of absorption. It is remarkable that a single complex square barrier allows us, for type I conditions, to achieve survivals below 10^{-7} in the studied range.

Other potentials do not behave as efficiently as the former group in the low k_0 region. In particular, the monomials with η real (types I or P) are useless for very low k_0. The linear potential improves somewhat the performance of the quadratic potential, but not enough to make it a practical option.

The absorption of the monomials improves substantially for I conditions by considering a complex prefactor as discussed in ref 10 and more recently in ref 16. However, this significant improvement is not achieved for type P potentials. (The curve for $V_{LC,P}$ has not been included since it is similar to the one for $V_{LR,P}$, except for $k_0 \leq 3$, where it is only slightly better.)

3.2. Absorption Width. Besides the optimized absorption at one particular k_0, the effective absorption width around k_0 is a very important parameter to determine the applicability of a potential. The effective absorption width $\Delta(k_0; \epsilon)$ is defined as the interval around k_0 where $S(k) \leq \epsilon$. Figure 4 shows this width for $\epsilon = 0.001$. For V_{QR} and V_{QC} we use the same potentials that have been optimized in Figure 1. Again, V_{QR} (squares) is useless at low momentum, but its effective width grows very rapidly from a certain threshold. In accordance with Figure 1, V_{QC} (circles) has a nonzero effective absorption width at low momenta only for type I potentials, but this width is rather small in any case. $V^{(2)}_{BMM}$ optimized potentials (triangles up) provide in comparison with the quadratic potentials larger absorption widths at low momenta, although their behavior at higher k_0 is deceptive. There is anyway some improvement by using type I conditions (with an infinite wall at $x = 1$) instead of type P conditions. By far the best performance is achieved with composite potentials V_{SB} formed by addition of square barriers. We have taken five barriers, $N = 5$, in the calculations of Figure 4 (diamonds), but the results may still improve by increasing N. Figure 4 is complemented by Figure 5, where

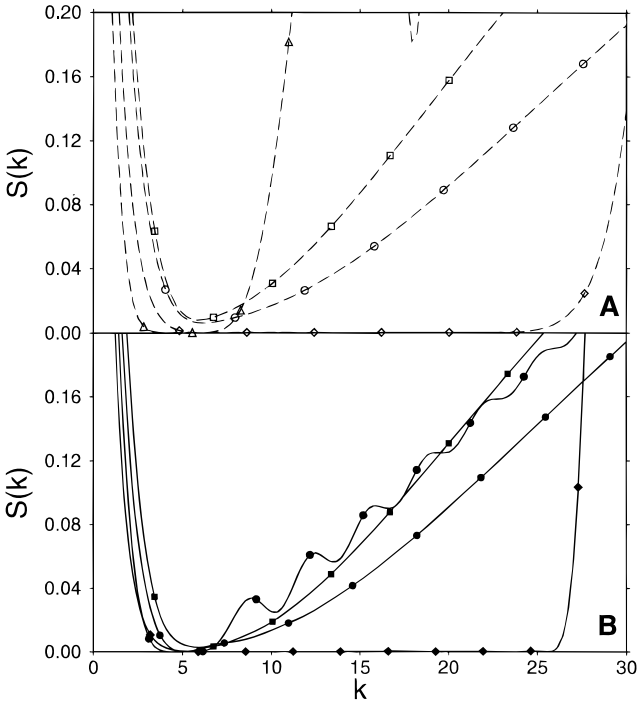

Figure 5. Survival curves $S(k)$ for the same potentials of Figure 4 optimized at $k_0 = 5$.

the survival curves $S(k)$ for the potentials optimized at $k_0 = 5$ are represented, and the important improvement of the composite potentials V_{SB} with respect to all other functional forms is made evident. The coefficients for each of the potentials of Figure 5 are given in Table 1. Moreover, Figure 3 represents the real and imaginary parts of the potential $V_{SB,I}(N = 5)$ used in Figure 5.

3.3. Robustness. Other valuable quality of a good absorber is the "robustness" versus discretization. To quantify the "robustness" of a given potential in a manner as independent as possible of any particular wave packet or calculational method, the following quantity will be used:

$$E_a(k_0) = S(k_0) - S_N(k_0) \tag{26}$$

where $S(k_0)$ is the survival for the selected potential and $S_N(k_0)$ is the survival for a discretized approximation of the original potential constructed by N square barriers of equal width δ, $N\delta = 1$. The barriers of the "discrete approximation" are chosen as

$$V_j = V(x_j) \qquad j = 1, ..., N \tag{27}$$

where $x_j = (j - {}^1/_2)\delta$.

Figure 6 represents the imaginary part of an arbitrary potential and its discretized version when $N = 5$. Using the transfer matrix technique the transmission and reflection coefficients for these square barrier potentials are obtained easily.[14] Figure 7 shows the absolute error E_a versus N for $k_0 = 1$. The three potentials examined in this figure, V_{QR}, V_{QC}, and $V^{(0)}_{BMM}$, are well represented with discretizations of seven or more barriers. A curious result is that the barrier approximation behaves better than the potential V_{QR}, although in this energy region this particular potential is not very effective; see again Figure 1. $V^{(0)}_{BMM,I}$ is quite robust, and its approximations with one or two barriers provide the smallest error among the potentials compared in Figure 7. On the contrary $V^{(2)}_{BMM}$ potentials oscillate too much and are not robust (their E_a is too large to be drawn in the scale of the figure.) With this robustness criterion the potentials V_{SB} formed by N_0 square barriers are perfectly robust when a multiple of N_0 is used in the discretization, $N = nN_0$, $n = 1, 2, 3, ...$, but for other values E_a can be significant. This means in practice that when discretizing the V_{SB} potentials on a grid, one should always put an integer number of points (typically 1, 2, or 3) for each square barrier to obtain good agreement with the theoretical absorption.

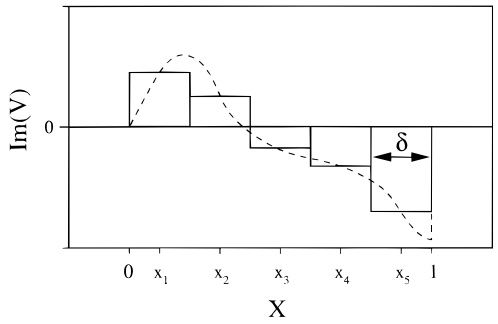

Figure 6. Imaginary part of an arbitrary potential and its discretized approximation with $N = 5$.

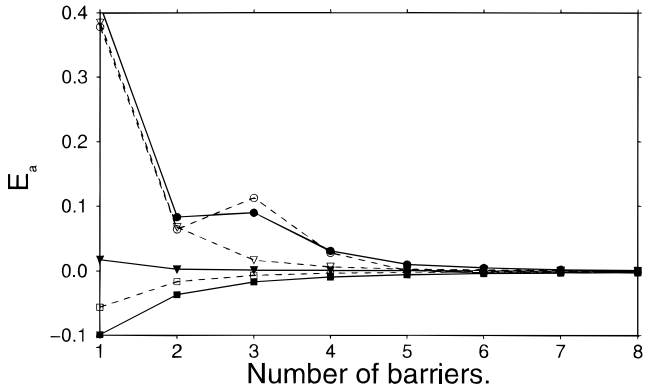

Figure 7. Absolute error of the survival, E_a, versus the number of discretization barriers for $k_0 = 1$. The lines are drawn as a visual aid (since only integer values make sense.) Triangles down, $V^{(0)}_{BMM}$; the rest of the symbols are as in Figure 4.

TABLE 1: Parameters for the Potentials of Figure 5

$V_{QR,I}$	$\eta_{QR} = (0.61419 \times 10^2, 0)$
$V_{QR,P}$	$\eta_{QR} = (0.11182 \times 10^3, 0)$
$V_{QC,I}$	$\eta_{QC} = (0.74360 \times 10^2, -0.52910 \times 10^2)$
$V_{QC,P}$	$\eta_{QC} = (0.15113 \times 10^3, -0.75050 \times 10^2)$
$V^{(2)}_{BMM,I}$	$a_0 = (1, 0)$
	$a_1 = (0, 5)$
	$a_2 = -a_0 - a_1 - a_3 - a_4$
	$a_3 = (0.29166 \times 10^2, -0.10395 \times 10^2)$
	$a_4 = (-0.12891 \times 10^2, 0.10522 \times 10^2)$
$V^{(2)}_{BMM,P}$	$a_0 = (1, 0)$
	$a_1 = (0, 5)$
	$a_2 = -3a_0 - 2a_1 + a_4 + 2a_5 + 3a_6 + 4a_7$
	$a_3 = 2a_0 + a_1 - 2a_4 - 3a_5 - 4a_6 - 5a_7$
	$a_4 = (0.23264 \times 10^4, 0.24091 \times 10^4)$
	$a_5 = (-0.40929 \times 10^4, -0.37388 \times 10^4)$
	$a_6 = (0.32269 \times 10^4, 0.27900 \times 10^4)$
	$a_7 = (-0.94918 \times 10^3, -0.80405 \times 10^3)$
$V_{SB,I}(N = 5)$	$V_1 = (-0.26953 \times 10^4, 0.73126 \times 10^3)$
	$V_2 = (-0.49506 \times 10^4, -0.66007 \times 10^2)$
	$V_3 = (-0.89834 \times 10^4, -0.24970 \times 10^4)$
	$V_4 = (-0.65683 \times 10^4, 0.43720 \times 10^3)$
	$V_5 = (-0.15653 \times 10^4, 0.67373 \times 10^3)$
$V_{SB,P}(N = 5)$	$V_1 = (-0.32005 \times 10^5, 0.19649 \times 10^4)$
	$V_2 = (-0.10844 \times 10^6, -0.18877 \times 10^4)$
	$V_3 = (-0.32519 \times 10^4, -0.33460 \times 10^3)$
	$V_4 = (-0.37319 \times 10^4, -0.29552 \times 10^4)$
	$V_5 = (-0.48302 \times 10^3, -0.28221 \times 10^4)$

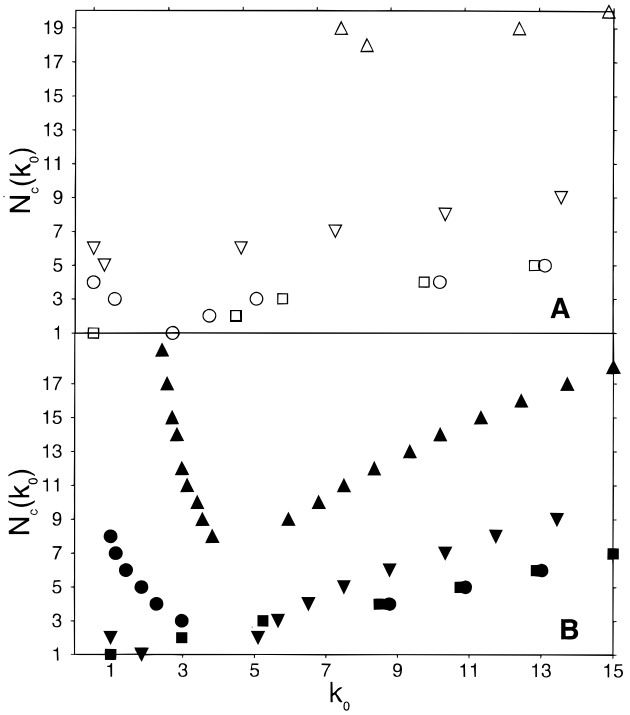

Figure 8. Number of barriers required so that $E_a \leq 0.001$ for potentials optimized at k_0 versus k_0 for type P conditions (A) or type I conditions (B). Triangles down, $V^{(0)}_{BMM}$; the rest of the symbols are as in Figure 4.

To examine the robustness as a function of the incident momentum we have defined $N_c(k_0)$ as the number of barriers required so that $E_a \leq 0.001$ for a potential optimized at k_0. As a general rule N_c increases with k_0 except possibly in the low momentum region. As indicated before, $V^{(2)}_{BMM}$ is not at all robust: see Figure 8.

4. Conclusions

Complex potentials are an important tool in different calculation methods in quantum reactive collisions, so their improvement and rational use may have an immediate impact in the accuracy of the results and the range of systems that can be studied. We have examined the performance of several forms of absorbing potentials, in particular their numerical robustness versus discretization and their effective absorption width when periodic or infinite barrier boundary conditions are imposed. (Both conditions are found in actual applications.) No single potential is useful for all purposes, but our study allows selection of the most adequate potential for each application. Besides absorption width and robustness, the stability of certain numerical methods requires that the potential satisfy additional properties. In particular, some of the time-dependent propagation algorithms are unstable when the imaginary part of the complex potential takes a large positive value. (We have noted this unstable behavior with the Caley transform or split propagation methods.) For these unstable methods the best choice will be among one of the following potentials: monomials, $V^{(0)}_{BMM}$, or V_{SB} with the restriction $Im\ (V_j) < 0$. Depending on the absorption interval, we may distinguish the following cases:

(a) Monochromatic absorption: In this case the best choice is $V^{(0)}_{BMM}$. This is an explicit (no optimization is required) and robust potential (in spite of the singularities), with a purely negative imaginary part, that will absorb at any chosen k_0, so that in dimensional units the potential length L may be arbitrary (in practice subject only to the restrictions imposed by robustness). The form for I conditions was known and in this work we have given the explicit form for P conditions. The monomials could be also used but they have a number of drawbacks. First of all the parameters have to be optimized. Second, in the low k_0 region they only absorb for I conditions and for a complex prefactor η.

(b) Broad momentum interval, $[k_i,k_f]$, with $k_i > 10$: In this case any monomial may be used efficiently. For simplicity, the linear potential V_{LR} may be recommended since the prefactor $\eta(k_0)$ can be easily estimated.[7,12] If a minimum, nonzero dimensional momentum p_i can be established for a particular application, the corresponding k_i can always be increased beyond $k \approx 10$ by increasing L, since $k = pL/\hbar$. However, this may lead to very large potential widths and consequently to a very heavy numerical burden. Accurate calculations at thresholds, or for low-energy scattering, would require extremely large (and impractical) values of L. An additional possible source of difficulties is that the robustness of the optimized monomials decreases when k_0 increases.

(c) Broad momentum interval including the region $k < 10$: At thresholds, for low-energy scattering, or to avoid too large values of the absorption length L, this is the important case. The best choice available is the composite potentials formed with square barriers, V_{SB}. These are very robust potentials provided each barrier is sampled with an integer number of discretization points. The optimization of the barrier energies can be constrained so that only negative imaginary parts are allowed[15] and any stability problem is avoided. In the cases where the algorithms are stable for potentials with positive imaginary parts, the constraint may be removed to obtain better absorption profiles.

Finally, our study provides sufficient examples that should also clarify a number of misconceptions about complex potentials that have at times hindered a more extensive search of functional forms: In particular, the absorbing potentials do not have to be purely imaginary (the addition of a real part adds flexibility and improves the absorption);[10,16] the potential width may be smaller than the incident momentum wavelength; and potentials with discontinuities do not necessarily cause reflection and can be numerically robust.

Acknowledgment. Many discussions with S. Brouard are acknowledged. The work has been supported by Gobierno Autónomo de Canarias (Spain) (Grant PB2/95) and Ministerio de Educación y Cultura (Spain) (PB 97-1482). J.P.P. acknowledges an FPI fellowship from Ministerio de Educación y Cultura.

References and Notes

(1) Kosloff, R.; Kosloff, D. *J. Comput. Phys.* **1986**, *63*, 363.
(2) Neuhauser, D.; Baer, M. *J. Chem. Phys.* **1990**, *92*, 3419.
(3) Seideman, T.; Miller, W. H. *J. Chem. Phys.* **1992**, *96*, 4412.
(4) Neuhauser, D. *J. Chem. Phys.* **1995**, *103*, 8513.
(5) Peng, T.; Zhang, Z. H. *J. Chem. Phys.* **1996**, *105*, 6072; *J. Chem. Phys.* **1997**, *106*, 1742.
(6) Balakrishnan, N.; Kalyanaraman, C.; Sathyamurthy, N. *Phys. Rep.* **1997**, *280*, 79.
(7) Neuhauser, D.; Baer, M. *J. Chem. Phys.* **1989**, *90*, 4351.
(8) Vibók, A.; Balint-Kurti, B. B. *J. Chem. Phys.* **1992**, *96*, 7615.
(9) Brouard, S.; Macías, D.; Muga, J. G. *J. Phys. A* **1994**, *27*, L439.
(10) Macías, D.; Brouard, S.; Muga, J. G. *Chem. Phys. Lett.* **1994**, *228*, 672.
(11) Riss, U. V.; Meyer, H. D. *J. Phys. B* **1995**, *28*, 1475.
(12) Riss, U. V.; Meyer, H. D. *J. Chem. Phys.* **1996**, *105*, 1409.
(13) Palao, J. P.; Muga, J. G.; Sala, R. *Phys. Rev. Lett.* **1998**, *80*, 5469.
(14) Kalotas, T. M.; Lee, A. R. *Am. J. Phys.* **1991**, *59*, 48.
(15) Palao, J. P.; Muga, J. G. *Chem. Phys. Lett.* In press.
(16) Ge, J. Y.; Zhang, J. Z. H. *J. Chem. Phys.* **1998**, *108*, 1429.